

FRACTURE OF LEAD-FREE SOLDER JOINTS AS A FUNCTION OF STRAIN RATE, LOCAL END GEOMETRY AND THICKNESS

Amir Nourani and Jan K. Spelt
University of Toronto
Toronto, ON, Canada
spelt@mie.utoronto.ca

ABSTRACT

The fracture of SAC305 solder was investigated as a function of strain rate using Cu-solder-Cu double cantilever beam (DCB) specimens joined with a series of 2 mm long discrete solder joints of 150 μ m thickness. The joints were then fractured with various strain rates under mode I and mixed-mode loading conditions. The failure of each joint in the DCB was accompanied by a sharp drop in the applied load. These maximum loads were used to calculate the initiation critical strain energy release rate, G_{ci} , of the solder joints using a finite element model. The results showed a substantial increase of about 75% in the solder joint fracture toughness at strain rates of 0.05 to 1 s^{-1} compared to that under quasi-static loading conditions. This trend suggests that the solder G_{ci} increases rapidly with strain rate whereas the G_{ci} of the IMC is relatively independent of strain rate. Negligible changes in G_{ci} were measured when the solder joint thickness was increased to 400 μ m. The dependence of crack initiation on the local shape of the solder joint at its end was investigated by fabricating the 2 mm long joints with either a square end (using Kapton tape) or a rounded end (using an embedded wire). Interestingly, these two local geometries produced almost identical values of G_{ci} , suggesting that initiation was not a strong function of the shape of the solder joint.

Key words: solder joint, strain rate, fracture test, strain energy release rate

INTRODUCTION

The reliability of solder joints under high strain rate loading conditions has been studied for many years, but the vast majority of testing has been qualitative, providing useful comparative data for specific solder joint materials and combinations of tensile and shear loads. The boardlevel drop test (BLDT) and the ball impact test (BIT) have been used to characterize the fracture behavior of BGA solder joints for different solder alloys [1,2]. The highspeed tensile test has been found to be a good method to characterize the fracture behavior of BGA solder joints and to evaluate the IMC strength that is effective under the actual impact loading conditions created by product drop [3,4].

Most of the studies measured solder joint strength for specific geometries, materials and loading conditions. Therefore, they may not be able to predict solder joint fracture strength at high strain rates for arbitrary joint geometries and loadings.

A systematic approach to predict solder joint strength under quasi-static loading has recently been developed [5,6]. This study tried to generalize the solder joint strength in terms of the strain energy release rate. The Rcurve behavior of cracks growing in relatively long SAC305 solder joints has been investigated in [5]. Cracks can form at a critical initiation strain energy release rate, G_{ci} , and then grow steadily to produce the rising part of an R-curve as the damage zone develops. A constant critical strain energy release rate, G_{cs} , is reached after a certain amount of subcritical crack growth [9], but quasi-static fracture load predictions for relatively short solder joints (e.g. less than 2 mm) could be made using G_{ci} , since crack growth was limited [8].

The current study extended the quasi-static approach of [6,7] to treat solder joint fracture under higher strain-rate loading conditions. Furthermore, a detailed study of some important manufacturing and fracture testing parameters of solder joints seems essential to be able to propose a high solder joint strength in microelectronic packages. Hence, the effect of local geometry and thickness of solder joint at higher strain rate loading conditions was also studied.

EXPERIMENTAL PROCEDURES

Specimen Preparation

Cu-solder-Cu double cantilever beam (DCB) specimens of 2 mm long discrete solder joints (Fig. 1) were prepared under standard surface mount (SMT) conditions as described in [6-8]. Prior to soldering, copper bars were polished using an ultra-fine silicon carbide/nylon mesh abrasive pad. This process produced a repeatable surface roughness very similar to that on commercial PCBs using an organic solderability preservative (OSP) surface finish [6]. The copper surfaces were rinsed with water, cleaned with cheese cloth and finally rinsed by acetone to be prepared for soldering. The surfaces which were not to be soldered were masked by Kapton tape which produced a smooth, square local geometry for discrete solder joints. A

number of specimens were fabricated using an embedded wire at the solder joint edge to change the local geometry though. A flux-cored Sn3.0Ag0.5Cu (SAC305) 0.75 mm solder wire was soldered to C110 copper bars (160×12.6×12.6 mm) placed on a hot plate at the temperature of 240-250 °C. The thickness of solder joints (150 μm and 400 μm) was controlled using three steel wires clamped between the copper bars (Fig. 1). The spacing wires between the individual solder joints prevented the premature loading of an adjacent joint as the preceding one was being fractured [9]. The time above liquidus (TAL) was set to 120 s. The specimen was then convectively cooled to room temperature.

Fracture Tests

Fracture tests were conducted on the load jig of Fig. 2, in which the locations of the link pins can be selected to control the forces F_1 and F_2 applied to each arm of the DCB as given in Eq. (1):

$$\frac{1}{s_2 \left(1 + \frac{s_3}{s_4} \right)} \quad (1)$$

where s_1 , s_2 , s_3 and s_4 are defined in Fig. 2 as the distances between pin centers. This allows a single DCB specimen to generate a range of mode ratios from pure mode I ($F_1=F_2$) to pure mode II ($F_1 \neq F_2$). A servo-electric testing machine with a maximum cross-head speed of 4.23 mm/s, was used to generate strain rates up to 1 s^{-1} . The strain rate under quasi-static loading was in the order of 10^{-5} as in [6]. As in ref. [6], it was found that, due to the lack of Rcurve toughening for 2 mm joints, the solder joint fractured immediately after crack initiation, and only one failure load could be measured for each joint. The failure load was evident as a sudden drop in the recorded load, and was acquired from the load cell output connected to a high-speed data acquisition (DAQ) board (NI PCI-6036E) with the frequency of 2 kHz.

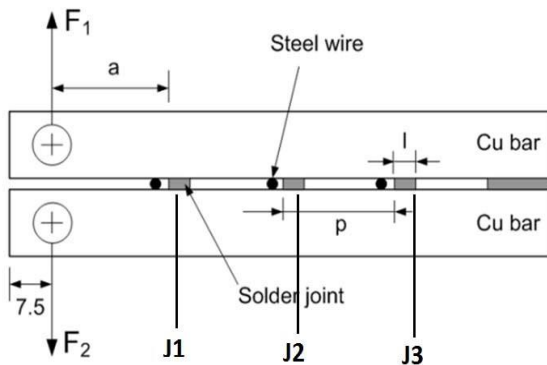


Figure 1. Fracture of discrete 2 mm joints to mimic the fracture aspects of small ball solder joints [7].

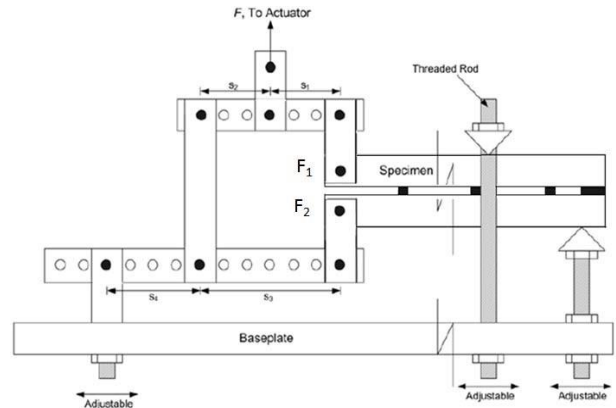


Figure 2. Schematic of the DCB specimen with discrete 2 mm long solder joints mounted in the mixed-mode load jig [7].

FINITE ELEMENT MODELS

G_{ci} Calculation

The failure loads on the specimen (F_1 and F_2) were used in a finite element model to calculate the critical strain energy release rate at crack initiation. In this study, G_{ci} represents the calculated critical initiation strain energy release rate where the solder is modeled as a linear elastic material.

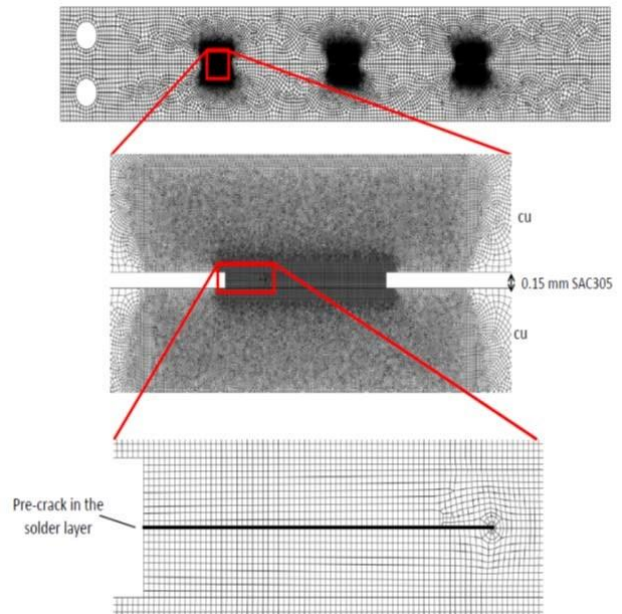


Figure 3. Typical finite element mesh to calculate G_{ci}

Two-dimensional plane stress elements and twodimensional plane strain elements were used to model the copper and solder, respectively.

The strain rate was not same for the three joints of one specimen since the distance from the loading pins changed. Since the mechanical properties of solder vary with the strain rate over this range, it was required to define the corresponding elastic modulus for each joint using the data for SAC305 in [6,10].

As in [6], a pre-crack of 500 μm was explicitly modeled in the middle of the solder layer to calculate the fracture toughness using the stress intensity factors to find G_{ci} (Fig. 3). The results were quite insensitive to the assumed initial crack length; e.g. a pre-crack length of 250 μm changed G_{ci} by less than 2.5%. The mesh size was smoothly changed from 0.0075 mm in the solder layer (20 elements in the thickness of solder) to 1 mm in the copper bars. The results were mesh size independent over this range. In each case, four contours around the crack tip were used to calculate the energy release rate. As expected, they produced almost path-independent G_{ci} values.

RESULTS AND DISCUSSION

Quasi-Static Loading

The fracture tests under quasi-static loading conditions on 400 μm thick SAC305 solder joints in mode I DCB yielded an average G_{ci} of $413 \pm 82 \text{ J/m}^2$ (95% confidence interval) for 10 data points obtained from 5 specimens and 10 individual joints. This was approximately the average value reported in [1] for the same solder and conditions (i.e. 380 J/m^2).

In comparison, the 150 μm thick SAC305 solder joints under mode I quasi-static loading on discrete 2 mm long, gave a mean value of $G_{ci}=433 \text{ J/m}^2 \pm 60 \text{ J/m}^2$ (95% confidence interval) for 14 data points, an increase of 5% compared to the mean G_{ci} of 400 μm thick solder joints. This difference in the fracture toughness between the 150 and 400 μm thick solder joints was not statistically significant (95% confidence). This is consistent with the results obtained in [8] where the fracture toughness did not change significantly when the solder joint thickness was changed from 400 μm to 200 μm . It is noted that the independence of the fracture toughness from the solder thickness is only true for relatively short solder joints, in which the ultimate fracture load is governed by the initiation strain energy release rate, G_{ci} , for which there is no R-curve toughening as cracks extend [8].

Loading at Higher Strain Rates - Mode I Fracture

Fracture tests of the same specimen were then performed at the maximum cross-head speed of 4.23 mm/s which produced a range of strain rates for the three joints in a single specimen depending on the load jig configuration. For

instance, when $s_1=s_2/2$ and $s_3=-s_4/2$, the first, second and third joints undergo strain rates of 0.3, 0.1 and 0.05 s^{-1} respectively. Strain rate was defined as:

$$\dot{l} / l_0 \quad (2)$$

where l_0 was the initial thickness of solder joint and dl/dt was the local rate of change of the solder layer thickness as calculated using the finite element model and the known rate of displacement of the ends of the specimen. Therefore, a range of strain rates were obtained by changing the cross-head speed and/or the location of loading pins in the load jig. Figure 4 shows the G_{ci} for these joints as a function of the strain rate calculated using FEA. Also shown is the quasi-static value obtained at a strain rate of approximately zero (10^{-5} s^{-1}).

The differences in G_{ci} values at strain rates between 0.05 and 1 s^{-1} were statistically insignificant (95% confidence). However, the mean strain energy release rate increased by a factor of 1.75 from the quasi-static value, $G_{ci}=433 \text{ J/m}^2$, to the average of the intermediate strain rate loading conditions, $G_{ci}=747 \text{ J/m}^2$ (Fig. 4).

Effect of Solder Joint Thickness on the Fracture Toughness

A number of tests were conducted to look into the effect of solder joint thickness on the initiation fracture toughness at strain rates between 0.05 and 1 s^{-1} . Although the mean G_{ci} increased from 749 J/m^2 for 150 μm thick solder joint to 843 J/m^2 for the 400 μm thick one, this difference was not statistically significant (95% confidence interval t -test) (Fig. 5). This is consistent with the earlier quasi-static observations of SAC305 solder joints where 0.2 mm and 0.4 mm thick solder joints were found to have almost identical fracture toughness at the same crosshead speed [8].

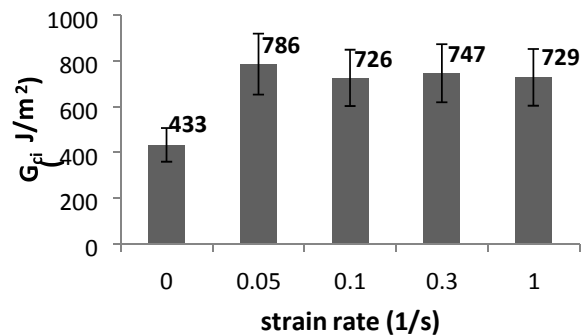


Figure 4. Comparison of initiation fracture toughness at different strain rates. From left to right, the number of data points for each strain rate were 14, 10, 7, 5 and 3,

respectively. Error bars show \square 95% confidence intervals.

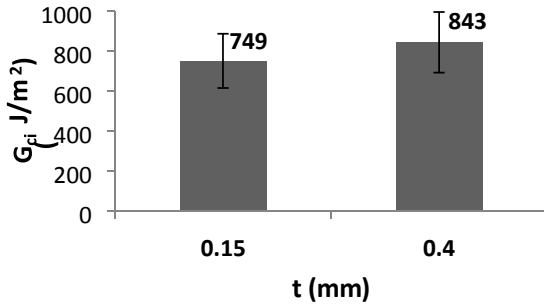


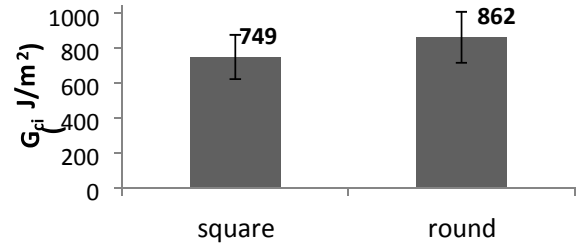
Figure 5. Effect of solder joint thickness on G_{ci} under intermediate strain rate loading. The difference is not statistically significant. 25 data points for 150 μ m-thick solder joint and 10 data points for 400 μ m-thick solder joint were obtained. Error bars show \square 95% confidence interval.

Effect of Local Geometry of Solder Joint on Fracture Toughness

As mentioned above, the local end geometry of most of the tested 2 mm solder joints was defined by Kapton tape which produced a square edge. Since this was quite different from the geometry of solder balls in BGAs, which can itself vary due to misalignments, it was of interest to gauge the sensitivity of G_{ci} to the local geometry of the end of the solder joint. Figure 6 illustrates the two end geometries that were used. Although the mean G_{ci} increased from 749 J/m² for square-end solder joints to 862 J/m² for round-end ones (Fig. 7), the difference was not statistically significant (95% confidence). This is similar to the observation in ref. [5] for the quasi-static testing of long continuous solder joints used in R-curve evaluations. This encouraging, because it means that fracture load predictions can, in principle, be quite accurate without the need for detailed modelling of **Figure 7.** Effect of solder joint local geometry on G_{ci} under intermediate strain rate loading. The difference was not statistically significant. 25 data points for square-end solder joint and 8 data points for round-end solder joint were obtained. Error bars show \square 95% confidence interval.

Fracture Load Prediction solder ball geometries.

The accuracy of fracture load predictions for the joints loaded at strain rates from 0.05 to 1 s⁻¹ was assessed by

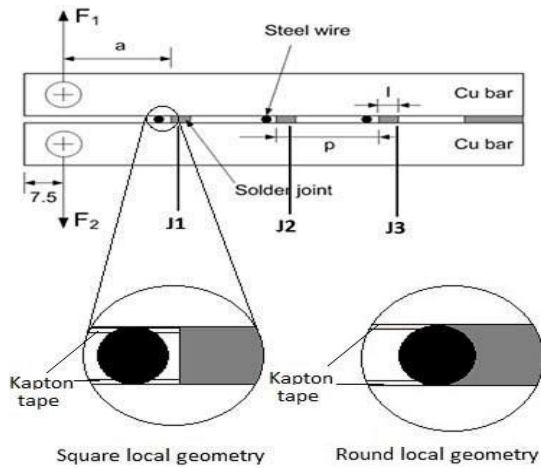


Solder

using the grand average value, $G_{ci}=747$ J/m², as a single failure criterion to calculate the failure loads for each of the DCB fracture tests. Table 1 shows that the average differences between these predictions and the measured fracture loads were quite small, with a maximum error of 8%. This is a promising conclusion that the generalized fracture load prediction of Cu-solder-Cu system can be extended from quasi-static to higher strain rate loading conditions. The strain energy release rate values obtained at different strain rates can be used to predict the corresponding failure loads of the same system at arbitrary geometries.

Table 1. Comparison of measured and predicted intermediate strain rate, mode I solder joint strengths. Failure criterion was $G_{ci}=747$ J/m².

Loading arm length, a (mm)	Strain rate (s ⁻¹)	Experimental load (N) (mean \pm standard deviation)	G_{ci} Prediction (N)	Difference
37	1	994 \pm 113	1013	2%
37	0.3	1010 \pm 117	1013	0.4%
74	0.1	527 \pm 74	569	8%
111	0.05	428 \pm 37	416	-3%



CONCLUSIONS

Variation in strain-rate can substantially change the initiation fracture toughness of lead-free solder joints.

Experiments on SAC305 solder joints showed that the

Figure 6. Two different tested local end geometries of critical crack initiation strain energy release rate, G_{ci} , solder joints increased by almost 75% when the loading rate was elevated from quasi-static (10^{-5} s^{-1}) to intermediate strain rates (0.05 to 1 s^{-1}). Variations in solder joint thickness and the local end geometry of the joints were found to have a negligible effect on G_{ci} at these strain rates. This is encouraging, since it should simplify fracture load predictions for actual solder joints in BGA and other components. For longer joints, however, R-curve toughening may cause a significant dependence of fracture toughness on solder thickness.

ACKNOWLEDGEMENTS

Funding for this research was provided by Blackberry and the Natural Sciences and Engineering Research Council of Canada. Valuable technical assistance and advice was provided by Dr. Gene Burger and Dr. Bev Christian at Blackberry.

REFERENCES

- [1] Lai YS, Yang PF, Yeh CL. Experimental studies of board-level reliability of chip-scale packages subjected to JEDEC drop test condition. *Microelectron Reliab* 2006;46:645-50.
- [2] Lai YS, Chang HC, Yeh CL. Evaluation of solder joint strengths under ball impact test. *Microelectronics Reliability* 2007;47:2179-87.
- [3] Lai A, Bradley E. Relationship of tensile interfacial strength to lead-free BGA impact performance. *Electronic Components and Technology Conference* 2006;1628-33.
- [4] Valota AT, Losavioa A, Renarc L, Vincenzo A. High speed pull test characterization of BGA solder joints. 7th. Int. Conf: on Thermal, Mechanical and Multiphysics Simulation and Experiments in Micro-Electronics and Micro-Systems, EuroSimE 2006:1-6.
- [5] Nadimpalli SPV, Spelt JK. R-curve behavior of Cu-Sn3.0Ag0.5Cu solder joints: Effect of mode ratio and microstructure. *Materials Science and Engineering: A* 2010;527:724-34.

- [6] Nadimpalli SPV, Spelt JK. Fracture load prediction of lead-free solder joints. *Eng Fract Mech* 2010;77:3446-61. [7] Nadimpalli SPV, Spelt JK. Mixed-mode fracture load prediction in lead-free solder joints. *Eng Fract Mech* 2011;78:317-33.
- [8] Nadimpalli SPV, Spelt JK. Effect of geometry on the fracture behavior of lead-free solder joints. *Eng Fract Mech* 2011;78: 1169–81.
- [9] Nadimpalli SPV. Characterization and Prediction of Fracture within Solder Joints and Circuit Boards. PhD thesis, University of Toronto 2010.
- [10] Wong E, Selvanayagam C, Seah S, Van Driel W, Caers J, Zhao X et al. Stress–strain characteristics of tinbased solder alloys for drop-impact modeling. *J Electron Mater* 2008;37:829-36.
- [11] Che F, Poh EC, Zhu W, Xiong B. Ag content effect on mechanical properties of Sn-xAg-0.5 Cu solders. *Electronics Packaging Technology Conference*, 2007:713-8.
- [12] Vianco PT, Rejent JA, Martin JJ. The compression stress-strain behavior of Sn-Ag-Cu solder. *JOM Journal of the Minerals, Metals and Materials Society* 2003;55:50-5.